Stability Requirements of Deep Steel Wide-Flange Columns under Cyclic Loading

Ahmed Elkady[1], Dimitrios G. Lignos[2]

Abstract
Just recently, valuable experimental data that characterized the hysteretic behavior of deep wide-flange steel columns (i.e., column depth, d >16 inches) at full-scale became available. Such members are typically used in steel moment-resisting frames (MRFs) in North America. In order to expand the findings of the experimental program, an extensive parametric study is conducted using a validated continuum finite element (FE) modeling approach. The nonlinear behavior of more than 40 steel wide-flange cross-sections is investigated. Each steel column is subjected to a monotonic, a symmetric cyclic, and a collapse-consistent lateral loading protocol coupled with different levels of constant compressive axial load ratios. Based on the FE results, the cyclic deterioration in the column flexural strength and stiffness is evaluated. Accordingly, design recommendations are developed related to the seismic compactness criteria for highly ductile members such that column axial shortening can be reduced under design basis and low-probability of occurrence earthquakes. The range of out-of-plane force demands is also evaluated for the lateral bracing design of columns in steel MRFs. In that respect, the current AISC provisions are evaluated. Empirical equations are developed for predicting the out-of-plane force demands and the plastic hinge length in steel wide flange columns.

1. Introduction

For the past fifty years, several experimental studies have investigated the monotonic and/or cyclic behavior of wide-flange/I-shaped steel columns (Popov et al. 1975; MacRae et al. 1990; Nakashima et al. 1990; Newell and Uang 2006; Chen et al. 2014; Suzuki and Lignos 2015). These studies mainly investigated columns with shallow cross-sections (i.e., depth less than 400mm). Nonetheless, deep wide-flange cross-sections are commonly used in columns of steel moment resisting frames (MRFs), designed in highly seismic regions in North America. Those deep cross-sections provide sufficient strength and stiffness to satisfy capacity design requirements according to the current seismic provisions (AISC 2010a). More specifically, deep and compact cross-sections with relatively large local slenderness ratios are employed in design in order to save steel weight. Consequently, their cyclic behavior under lateral drifts, combined with compressive axial load becomes questionable. Notably, NIST (2010) established a research

---

[1] Post-Doctoral Researcher, Swiss Federal Institute of Technology, Lausanne, <ahmed.elkady@epfl.ch>
[2] Associate Professor, Swiss Federal Institute of Technology, Lausanne, <dimitrios.lignos@epfl.ch>

plan that highlighted the need for further research related to the hysteretic behavior of deep wide-flange beam-columns as part of steel MRFs under earthquake loading.

To address this issue, full-scale testing of deep wide-flange columns was conducted recently. In particular, Uang et al. (2015) tested 25 W24 steel column specimens. The specimens were 5.5 meters long and had fixed boundary conditions at both column ends. The majority of the specimens were subjected to unidirectional symmetric lateral loading protocol combined with different levels of constant compressive axial load ranging from 20% to 60% P_y, where P_y is the axial yield strength. These tests showed that local buckling or lateral torsional buckling could dominate the column behavior depending on its local and global slenderness. However, the observed lateral torsional buckling failure modes might be influenced by the simplified boundary conditions incorporated in those tests (i.e., fixed-fixed boundary conditions). Furthermore, the effects of bidirectional loading and lateral loading history on the behavior of nominally identical column specimens were not thoroughly investigated. A second experimental program was conducted by the authors, Elkady and Lignos (2016, 2017), in which ten, 3.9 meters-long, W24 steel column specimens were tested. Most of the specimens had a fixed base, and flexible boundary conditions at the top column end in order to realistically capture the flexibility of the beam-to-column joint. The specimens were subjected to unidirectional/bidirectional symmetric and collapse-consistent lateral loading protocols combined with a constant compressive axial load of 20% P_y. Those two testing programs showed that compact cross-sections with web and flange slenderness ratios, close to the compactness limits specified by AISC (2010a) for highly ductile members (λ_{hd}), can deteriorate fairly rapidly in flexural strength and stiffness. In particular, these cross-sections can lose 20% of their maximum flexural capacity at chord-rotations less than 3% radians due to severe local buckling. Other failure modes were also observed such as column axial shortening, out-of-plane column deformations exacerbated at the center of local buckle near the column base. Lateral torsional buckling was a secondary failure mode in columns with relatively large member slenderness ratios.
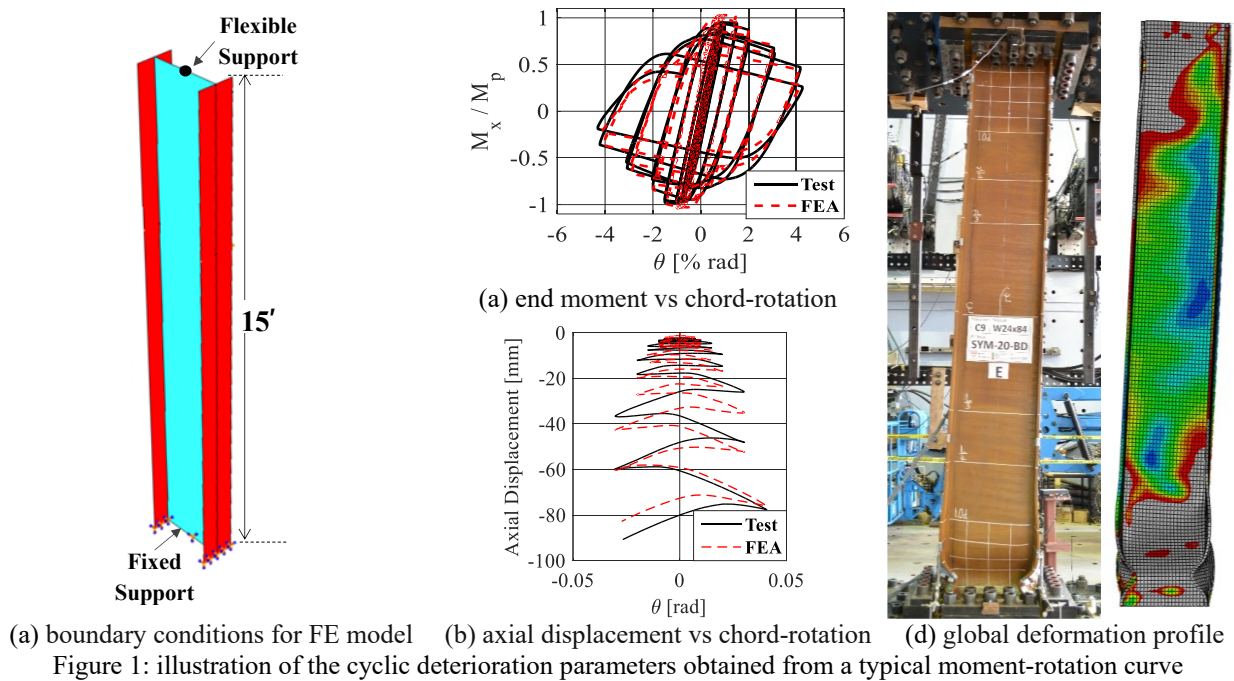
The aforementioned experimental studies provided valuable data on the hysteretic behavior of deep wide-flange columns under multi-axis cyclic loading. Nonetheless, the experimental data remain limited with respect to the number of investigated cross-section sizes and the applied axial load levels. In order to develop recommendations for stability requirements of deep wide-flange columns, a wide range of cross-sections need to be investigated. To this end, a parametric study, that utilizes a thoroughly validated finite element (FE) modeling approach, is conducted in order to expand the findings of the experimental studies. In particular, the hysteretic behavior of more than 40 wide-flange cross-sections is investigated as part of a typical first-story interior MRF column. The large pool of data generated by the parametric study is then used to develop design recommendations for such members. These recommendations aim to limit the level of strength and stiffness deterioration in MRF columns. Additionally, the out-of-plane force demands at the column top as well as the plastic hinge length at the column base are evaluated. Empirical equations that relate those two parameters to the cross-section's geometric properties are developed.

2. Finite Element Model Specifics and Parametric Study
A parametric finite element (FE) study is conducted using the commercial software ABAQUS CAE (ABAQUS-FEA/CAE 2011). The parametric study includes 40 wide-flange cross-sections

ranging from W16 to W36. The majority of the cross-sections are compact as per AISC (2010a) for highly ductile members (λ_{hd}), except for five cross-sections that satisfy the limits for moderately ductile members (λ_{md}). Unidirectional symmetric and collapse-consistent lateral loading protocols combined with four different levels of axial load of 0, 20, 35, and 50% P_y were incorporated in this study. Due to brevity, only the results of the symmetric loading protocol cases are discussed in this paper. The utilized unidirectional symmetric protocol (noted here as the SYM protocol) is the one developed by Clark et al. (1997) and utilized by AISC (2010a) for the qualification of beam-to-column connections. The complete list of cross-sections as well as other details of the parametric study can be found in Elkady and Lignos (2015a) and Elkady (2016).

The 40 cross-sections are investigated as part of a 15 ft (4.6m) steel column as shown in Fig. 1a. The column has a fixed base and flexible rotational boundary conditions at its top end in the strong-axis direction. Such boundary conditions are expected in a first-story interior MRF column. The FE model is meshed using shell elements to better capture severe local buckling. The shell elements are assigned a nonlinear kinematic/isotropic material model representative of standard A992 Gr. 50 (ASTM 2015) steel material with an expected yield strength of 380MPa (55 ksi). Local and global geometric imperfections as well as residual stresses were incorporated in the FE model. The FE model was thoroughly validated against past experimental data on small and stocky columns (MacRae et al. 1990; Newell and Uang 2006) as well recent data on deep and slender columns (Uang et al. 2015; Elkady and Lignos 2016, 2017). Figures 1b to 1d show a sample comparisons between the FE simulations and the test data from Elkady and Lignos (2016). Further details on the FE modeling approach and its validation can be found in Elkady and Lignos (2015a) and Elkady (2016).

(a) boundary conditions for FE model (b) axial displacement vs chord-rotation (d) global deformation profile

Figure 1: illustration of the cyclic deterioration parameters obtained from a typical moment-rotation curve

2. Discussion

A total of 160 data sets are obtained from the parametric study (40 cross-sections x 1 lateral loading protocol x 4 axial load levels). The typical hysteretic behavior of a steel column, in terms of the end moment at the column base versus chord-rotation, under symmetric lateral loading is shown in Fig. 2. In the same figure, the moment-rotation relation is fitted with a first-cycle envelope curve. Two main parameters representing the cyclic deterioration in strength and stiffness are deduced from the moment-rotation data and discussed in the subsequent sections of this paper. The first parameter one is the chord-rotation at which 20% of the column's plastic flexural capacity, M_p, is lost ($\theta_{80\%Mp}$). This parameter is an indicator of how fast the column's flexural strength deteriorates cyclically due to local and global geometric instabilities. The second parameter is the unloading flexural stiffness at a chord-rotation i (K_i). This parameter is an indicator of how fast the column's flexural stiffness deteriorates cyclically due to member geometric instabilities (i.e., twisting and lateral torsional buckling).

To facilitate the interpretation of the FE results, the 40 cross-sections are divided into four sets based on the corresponding web and flange local slenderness ratios. Sets W1 represents cross-sections with the lowest flange and web slenderness ratios ($12.1 \leq h/t_w \leq 22$ and $2.15 \leq b_f/2t_f \leq 3.9$). Set W2 represents cross-sections with moderate local slenderness ratios ($22 \leq h/t_w \leq 32.5$ and $3.9 \leq b_f/2t_f \leq 5.5$). Set W3 represent cross-sections with local slenderness ratios close to λ_{hd} limits according to AISC (2010a) ($32.5 \leq h/t_w \leq 43$ and $5.5 \leq b_f/2t_f \leq 7.0$). Set W4 represents the five compact cross-sections with local slenderness ratios close to λ_{md} limits according to AISC (2010a) ($43 \leq h/t_w \leq 57.5$ and $7 \leq b_f/2t_f \leq 8.5$).
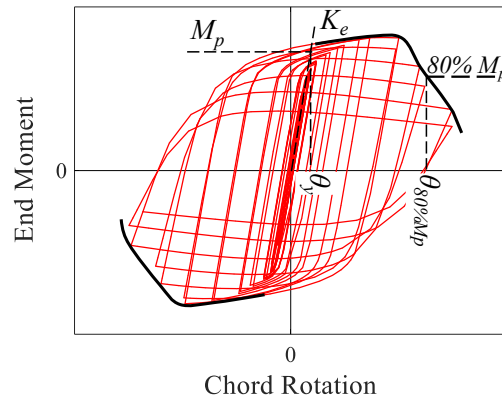

Figure 2: illustration of the cyclic deterioration parameters obtained from a typical moment-rotation curve

2.1 Cyclic Deterioration in Flexural Strength

The current seismic provisions in North America (CSA 2009; AISC 2010a) do not specify any recommendations with respect to the allowable level of cyclic deterioration in flexural strength in steel columns. Nonetheless, pre-qualified fully restrained beam-to-column connections should maintain 80% of the beam's plastic flexural strength at a chord-rotation of 4% radians when subjected to a symmetric cyclic protocol. Using this criterion as a reference, the column hysteretic behavior is assessed. In Fig. 3, the chord-rotation at which 80% M_p is reached is plotted with respect to the web slenderness ratio (h/t_w) for all 40 cross-sections for the load cases with axial load level of 20% and 50% P_y. In the same figure, the web compactness limit for highly ductile members, λ_{hd}, as per AISC (2010a) is superimposed considering an axial load ratio of 50% P_y. Note here that plastic flexural strength, M_p, is calculated by neglecting the axial load-flexural interaction.

4

Figure 3 shows that cross-sections with larger web slenderness ratio reach 80% of their M_p at lower chord-rotations compared to those with stockier webs. This observation holds true with respect to the flange slenderness ratio. In particular, at 20% P_y, only cross-sections with relatively small web slenderness ratios (i.e., Sets W1 and W2: h/t_w ≤30) reach a chord-rotation of 4% radians while maintaining 80% M_p. On the other hand, the least compact cross-sections with web slenderness ratios close to λ_{hd} (i.e., Set W3: 32.5≤ h/t_w ≤43) reach 80% M_p at a chord-rotation of about 2% radians. This issue becomes more critical at higher axial load ratios as shown in Fig. 3b for the 50% P_y load case. This is attributed to the early onset of local buckling (i.e., onset of flexural strength deterioration) under higher axial load ratios. It should be noted that a constant compressive axial load ratio of 20% to 35% P_y is expected in interior first-story columns of new steel frame buildings (Suzuki and Lignos 2014). Higher axial load ratios of magnitude 50% P_y and higher are expected in older steel frame buildings (Bech et al. 2015).

Based on the aforementioned results, a reduction to about two-thirds of the current compactness limit for highly ductile members (λ_{hd}) seems to be reasonable for steel columns with cross-sections that are relatively close to the current limit for highly ductile members (i.e., set W3) to achieve a chord-rotation of 4% radians with a reduction in column flexural strength of no more than 20% M_p. Such recommendation should be applicable for first story columns that plastification at their base is to be expected according to capacity design principles. This recommendation conforms with the incorporation of a higher strong-column-weak-beam ratio in steel special moment frames (SMFs) to reduce their collapse risk (Elkady and Lignos 2014, 2015b).
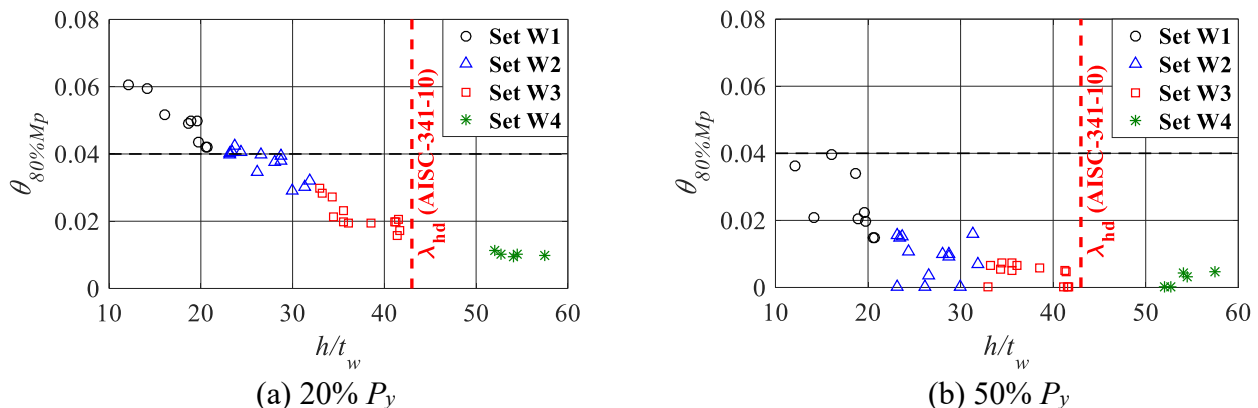

(a) 20% P_y (b) 50% P_y

Figure 3: Chord-rotation at 80% M_p versus web slenderness ratio for steel wide-flange beam-columns subjected to a symmetric cyclic loading protocol

2.2 Cyclic Deterioration in Flexural Stiffness

Out-of-plane member instability as well as twisting and lateral torsional buckling (called global instabilities from this point on) was observed in recent experimental programs that investigated the hysteretic behavior of deep and slender wide-flange columns. Such failure modes were more evident in columns with relatively large local and global slenderness ratios. To further investigate this issue, the unloading flexural stiffness due to global instabilities, is evaluated at each cycle (see Fig. 2). Figure 4 shows the flexural stiffness, normalized by the elastic flexural stiffness K_e, with respect to the cumulative inelastic rotation for all 40 cross-sections subjected to

20% and 50% P_y. At a given drift, the cumulative inelastic rotation $\Sigma\theta_H$ is calculated as the sum of absolute inelastic drift excursions following the yield drift rotation of the respective column, considering the axial load. In Fig. 4, two lines are superimposed at $\Sigma\theta_H$ =0.2 and $\Sigma\theta_H$ =0.6 rads. Those two $\Sigma\theta_H$ values correspond roughly to the second cycle at 2% and 4% radians of the symmetric cyclic loading protocol.

Figure 4 shows that columns with stocky cross-sections (i.e., Set W1: h/t_w ≤22) maintain their elastic stiffness (i.e., K/K_e ≤ 0.80) up to the second 2% drift cycle, regardless of the axial load ratio. However, the same columns can only maintain their elastic stiffness at the 4% drift cycle, if the axial load ratio is less than 35% P_y. On the other hand, columns that utilize cross-sections near the current compactness limits for highly ductile members (i.e., Set W3: 32.5≤ h/t_w ≤43) experience more than 50% loss in their original flexural stiffness at the second 2% drift cycle (i.e., $\Sigma\theta_H$ =0.2) when the applied axial load ratio is larger than 35% P_y. Note that a drift demand of 2% rads should be expected in steel MRFs during a design-basis seismic event. In that respect, the current allowable limit of 30% P_y for columns as part of steel MRFs based on the Canadian seismic provisions (CSA 2009) is rational. Note that a similar limit is not currently implemented in the (AISC 2010a) seismic provisions for new construction.

At 4% rads, the least compact columns (i.e., Set W3) lose about 80% of their elastic flexural stiffness even at an axial load ratio of 20% P_y. Note that a reduction in flexural stiffness larger than 50% is associated with severe global instabilities followed by an exponential increase in column axial shortening due to P-Delta effects. This is consistent with observations from full-scale tests by Elkady and Lignos (2016, 2017). A two-third reduction in the current AISC (2010a) seismic compactness limits for highly ductile members, limits the expected flexural stiffness reduction of columns to 51%, on average at 4% rads when the applied axial load ratio is 20% P_y (see Fig. 4a) Such drift amplitudes are associated with low probability of occurrence earthquakes. Such seismic events typically involve lesser number of inelastic cycles compared to those imposed by a symmetric lateral protocol (Krawinkler 2009; Lignos et al. 2013).
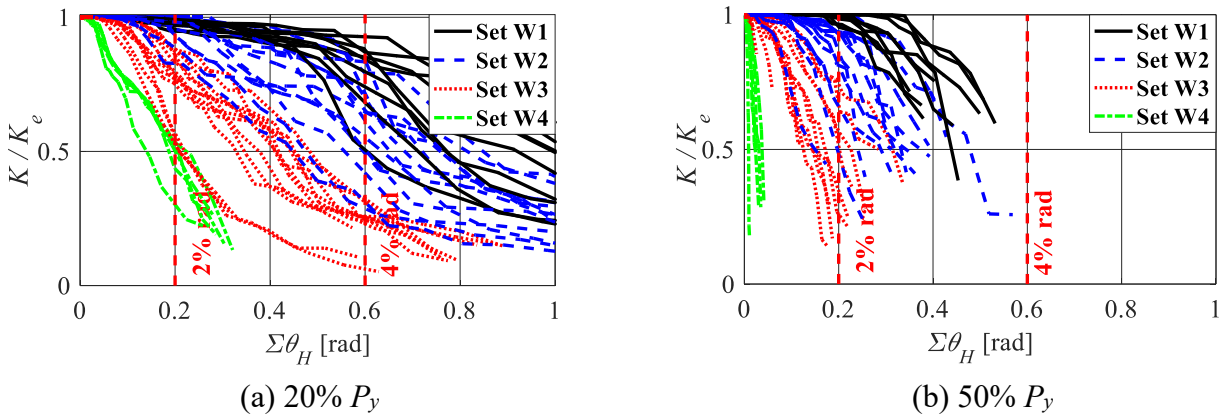

(a) 20% P_y (b) 50% P_y

Figure 4: Normalized unloading flexural stiffness versus cumulative inelastic rotation for beam-columns subjected to symmetric loading protocol

The cyclic deterioration in flexural stiffness is also dependent on the member slenderness, L_b/r_y, in which L_b is the laterally unsupported length of the column (i.e., L_b=4.6m) and r_y is the weak-axis radius of gyration of the cross-section. Figure 5a and 5b shows the normalized unloading

flexural stiffness (K/K_e) measured at $\Sigma\theta_H$=0.2 radians with respect to L_b/r_y, when the columns are subjected to 20% and 35% P_y, respectively. This figure shows that, at compressive axial loads less than or equal 35% P_y, columns with global slenderness ratios less than 80 seem to maintain at least 50% of their elastic flexural stiffness. This shows that the current L_b/r_y limit of about 50~60 specified by CSA S16-09 (CSA 2009) for columns as part of Type-D MRFs, may be overly conservative. Furthermore, it should be noted that cyclic deterioration in flexural stiffness is also dependent on the warping and torsional constants (C_w and J) of the cross-section. Therefore, one should consider appropriate warping and torsional constants in addition to an L/r_y limit. Based on this parametric study, the lower bound limits of $C_w \geq 5.4 \times 10^{13}$ mm^6 and $J \geq 2.3 \times 10^7$ mm^4 are recommended for highly ductile columns.

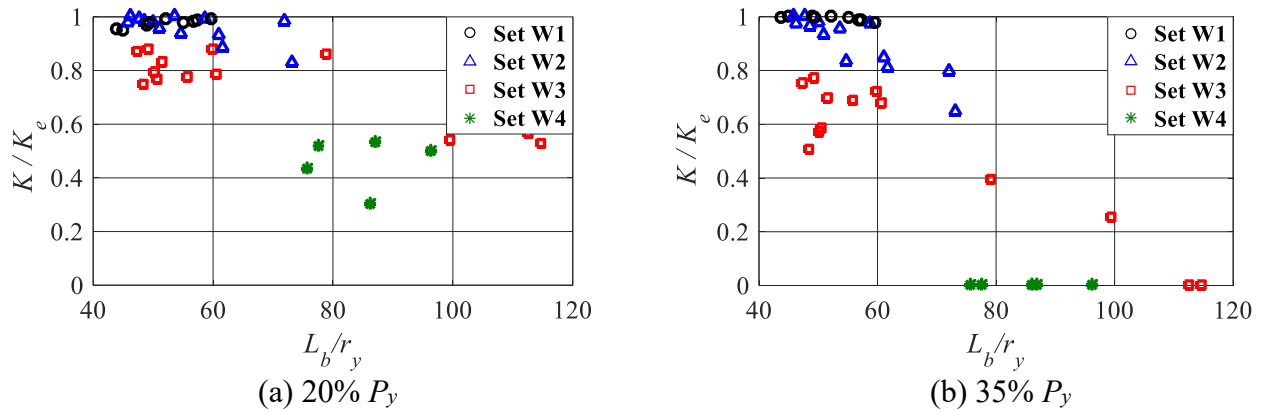

(a) 20% P_y (b) 35% P_y

Figure 5: Normalized unloading flexural stiffness measured at $\Sigma\theta_H$=0.2 rads (2% drift amplitude) versus global slenderness ratio for beam-columns subjected to symmetric loading protocol

2.3 Column Axial Shortening under Cyclic Loading

From the onset of local buckling, column axial shortening increases exponentially with the subsequent inelastic cycles. Axial shortening is an important failure mode, particularly in columns under relatively large compressive axial loads. This issue becomes more critical in high-rise steel frame buildings, where differential axial shortening levels between interior and exterior columns can lead to global structural instability. To this end, the recommendations discussed in the previous sections aim to limit the amount of axial shortening as well as the amount of cyclic deterioration in flexural strength and stiffness. To illustrate that, Fig.6 shows the progression of axial shortening (Δ_{axial}) normalized with respect to the column undeformed length L, versus the cumulative inelastic rotation for P/P_y = 20% (see Fig. 6a) and 50% (see Fig. 6b). This figure shows that at a 2% drift amplitude, all columns with P/P_y=20% and highly ductile cross-sections (i.e., Set W1, W2, and W3) shorten by less than 0.7% L. For axial load levels larger than 20% P_y, column axial shortening exceeds 1% L when the least compact cross-sections (i.e., Set W3) are utilized. Note that, even at axial load ratios less than 20% P_y, an axial shortening ratio larger than 1% L is also developed in all columns at 4% drift amplitude. Recent full-scale tests by Elkady and Lignos (2016, 2017) showed that when axial shortening exceeds 1% L, global instabilities start to develop rapidly. To this end, to achieve an axial shortening level less than 1% L at drift levels associated with design-basis seismic events (i.e., 2% rads), the current compactness limits need to be reduced by two-thirds and the axial load demands need to be limited to 30% P_y.
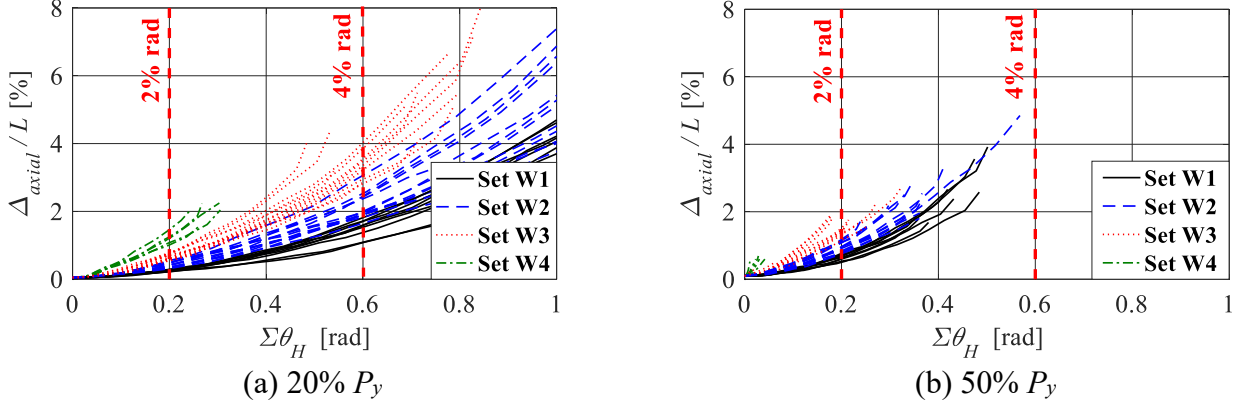
7

(a) 20% P_y (b) 50% P_y

Figure 6: Normalized beam-column axial shortening versus cumulative inelastic rotation subjected to symmetric loading protocol

2.3 Plastic Hinge Length

Steel frame modelers commonly utilize the "concentrated plasticity approach" when modeling steel columns. This approach assumes that plastification (i.e., nonlinear behavior) occurs at single points, typically allocated at the column ends. This assumption however can be inaccurate. Full-scale testing by Elkady and Lignos (2016, 2017) as well as recent tests from Suzuki and Lignos (2015) and Lignos et al. (2016) showed that columns can develop a plastic hinge length in the range 1.25 d to 1.9 d, measured from the column base, where d is the cross-section depth.

In the context of this paper, the plastic hinge length at the column base is evaluated based on the parametric FE study. The plastic hinge length is defined here as the distance between the column base and the last cross-sectional level with plastic strains. Figure 7 shows the plastic hinge length (L_{PH}), normalized by d, with respect to the web slenderness ratio for the load cases with an axial load ratio of 20% and 50% P_y. Note that in Fig. 7, L_{PH} is evaluated at the point when the column lost its flexural strength. This figure shows that a column that utilizes more compact cross-sections (ex. Set W1) develop a larger plastic hinge length of about 2.0 d compared to 1.0 d for those with the more slender cross-sections (ex. Set W4). This is attributed to the fact that it takes several inelastic cycles for local buckling to localize in stocky cross-sections; therefore, plastic strains spread over a larger length. Furthermore, under higher axial load ratios, columns develop larger plastic hinge lengths due to the second-order P-Delta effects. For example, an increase in the axial load ratio from 20% to 50% P_y resulted in an average 15% increase in the plastic hinge length (see Fig. 7a and 7b). It is important to point out that the observed increase in the plastic hinge length from the onset of local buckling till the point that the column reaches to zero flexural strength is 30%, on average.

Using the scatter of data shown in Fig. 7, a preliminary multivariate regression equation is developed to estimate the plastic hinge length for steel wide-flange columns. The multivariate regression equation is given by Eq.1,

$$\frac{L_{PH}}{d} = 1.837 \left(\frac{h}{t_w} \right)^{-0.443} \left(\frac{L_b}{r_y} \right)^{0.287} \left(1 - \frac{P}{P_y} \right)^{-0.259}, R^2 = 0.684, COV = 0.192 \qquad (1)$$

8

The range of applicability of Eq. 1 is: $12.1 \leq h/t_w \leq 57.5$, $44 \leq L_b/r_y \leq 120$, and $0 \leq P/P_y \leq 0.75$. This equation predicts the plastic hinge length with a coefficient of determination $R^2 = 0.561$ and a coefficient of variation, $COV = 0.141$. Based on Eq. 1, the plastic hinge length is dependent on the cross-section web slenderness ratio (h/t_w), the member global slenderness ratio (L_b/r_y) and the axial load ratio (P/P_y). It should be noted that L_{PH} is also dependent on the flange slenderness ratio ($b_f/2t_f$), however, since there is strong co-linearity between h/t_w and $b_f/2t_f$, only h/t_w is considered in Eq. 1 because it leads to an increased R^2. Kemp (1996) also developed an empirical formula for predicting the plastic hinge length. However, this formula was found to be adequate for cross-sections with relatively high local slenderness ratios (i.e., $32.5 \leq h/t_w \leq 57.5$ and $5.5 \leq b_f/2t_f \leq 8.5$). The same formula highly overestimated the column plastic hinge length for highly and moderately ductile cross-sections ($h/t_w \leq 32.5$ and $b_f/2t_f \leq 5.5$).
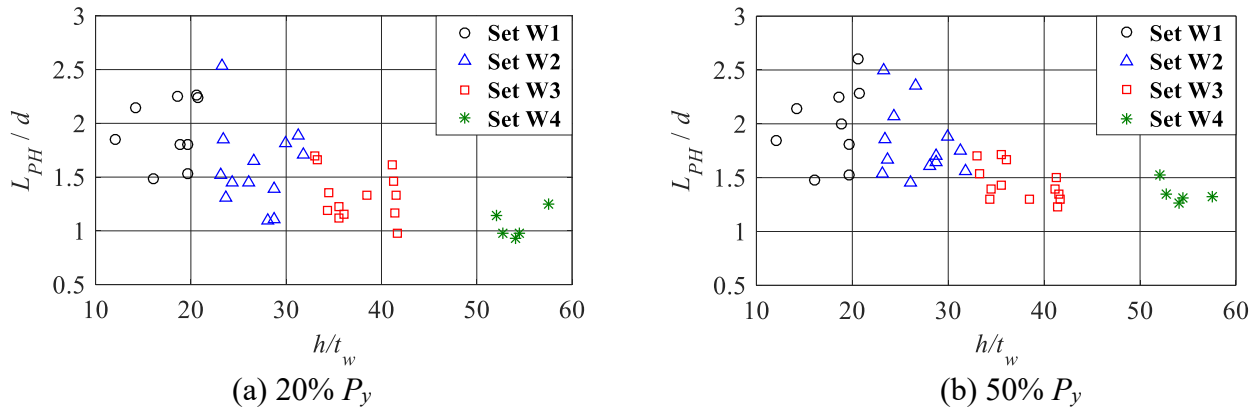

(a) 20% P_y (b) 50% P_y

Figure 7: Normalized plastic hinge length versus web slenderness ratio subjected to symmetric loading protocol

2.3 Out-of-Plane Force Demands

Recently, Elkady and Lignos (2016) monitored the out-of-plane force demands in full-scale deep column specimens (W610x125 and W610x217) subjected to multi-axis cyclic loading. It was observed that columns with local slenderness near the λ_{hd} limit can develop an out-of-plane force demand up to 2% P_y. It was also shown that the current steel specifications in North America, (CSA 2009; AISC 2010b), underestimate the lateral bracing design axial force for columns that experience lateral drift ratios larger than 4% radians. On the other hand, the lateral bracing axial force design requirements per CSA (2009) and AISC (2010b) was shown to be fairly conservative for columns with local and global slenderness ratios of $h/t_w \sim 47$ and $L_b/r_y \sim 80$, respectively.

The out-of-plane force demands at the column top are further investigated based on the parametric FE study. Figure 8 shows the relation between the out-of-plane force (P_{brace}), normalized by P_y, and the global slenderness ration (L_b/r_y) for the load cases with 20% and 50% P_y. Note that the reported P_{brace} values represent the maximum force measured up to a chord-rotation of 4% radians. In the same figure, the he lateral bracing axial force design requirements per CSA (2009) and AISC (2010b) are superimposed. This figure shows that the out-of-plane force is inversely proportional to the column's local and global slenderness ratios. Figure 8 also suggests that both CSA (2009) and AISC (2010b) overestimate the lateral bracing design axial force for columns with $L_b/r_y > 60$. In the same time, margin of safety against exceeding design brace force for columns with $L_b/r_y < 45$ is small. This shows that CSA (2009) and AISC (2010b)

9

design equations needs to be revisited. To this end, a preliminary expression is developed to estimate the out-of-plane brace force (P_{brace}) for wide-flange steel beam-columns. This expression represents the upper-bound value of P_{brace} based on three distinctive L_b/r_y regions (see Fig. 8). The expression is as follows:

$$\frac{P_{brace}}{P_y} = \begin{cases} 0.01\,C_a P_y & L_b/r_y < 45 \\ (0.025 + 3.3 \times 10^{-4} L_b/r_y)C_a P_y & 45 < L_b/r_y < 60 \\ 0.005\,C_a P_y & L_b/r_y > 60 \end{cases} \tag{2}$$

$$where,\ C_a = 0.75 + 1.33\,P/P_y$$

The range of applicability of this expression is: $12.1 \leq h/t_w \leq 57.5$, $44 \leq L_b/r_y \leq 120$, and $0 < P/P_y \leq 0.75$; in which the out-of-plane brace force depends on the global slenderness ratio (L_b/r_y) and the applied axial load ratio (P/P_y).
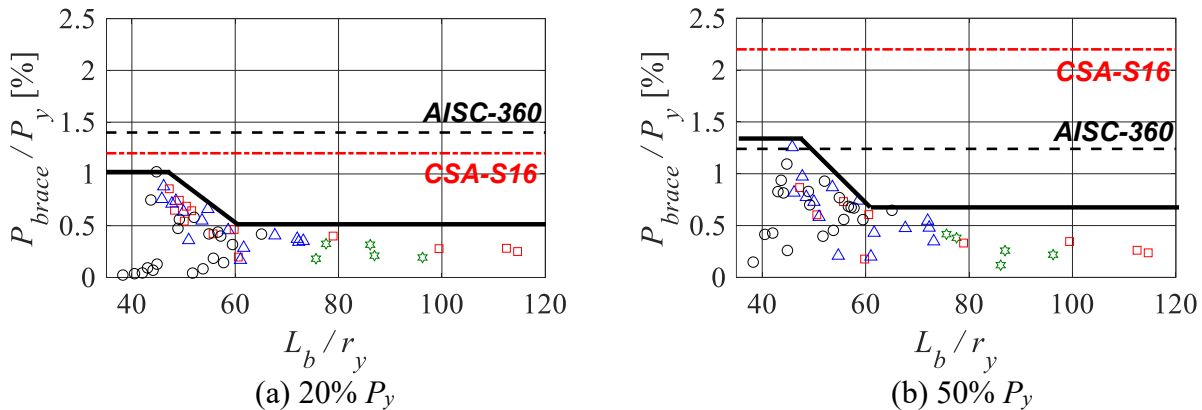

(a) 20% P_y (b) 50% P_y

Figure 8: Normalized brace force versus global slenderness ratio for wide-flange beam-columns subjected to symmetric loading protocol

3. Conclusions

A parametric analytical study was utilized to investigate the cyclic behavior of deep wide-flange steel columns typically used in steel MRFs designed in North America. The study utilized a robust and thoroughly validated finite element (FE) modeling approach. A total of 40 wide-flange cross-sections were investigated as part of a typical first-story MRF column. The loading protocol involved a symmetric lateral loading protocol coupled with different levels of compressive axial load ratios ranging from 0% to 50% P_y. The main findings are summarized as follows:

- Columns that utilize slender but seismically compact cross-sections ($32.5 \leq h/t_w \leq 43$ and $5.5 \leq b_f/2t_f \leq 7$), develop a total plastic rotational capacity less than 4% radians when subjected to 20% P_y. At $P/P_y=50\%$, the same columns reach 80% M_p at chord-rotations less than 1% radians.
- After the onset of local buckling, the column axial shortening increases exponentially with respect to the cumulative inelastic rotation. At $P/P_y=20\%$ and $\theta=4\%$ rads, columns that utilized cross-sections near λ_{hd} limits as per AISC (2010a) ($32.5 \leq h/t_w \leq 43$ and $5.5 \leq b_f/2t_f \leq 7$) shorten by about 6% L.

- Highly compact cross-sections developed a larger plastic hinge length of about 2.0 d compared to 1.6 d for the least compact cross-sections that were examined ($32.5 \leq h/t_w \leq 43$ and $5.5 \leq b_f/2t_f \leq 7$). The effect of the applied axial load on the plastic hinge length was found to be minor (i.e., 15% increase in plastic hinge length for an axial load increase from 20% to 50% P_y).
- Columns with global slenderness ratios, $L_b/r_y > 80$ experienced more than 50% reduction in their elastic flexural stiffness (K_e) at lateral drift demands associated with design-basis seismic events (i.e., 2% radians). This is due to global geometric instabilities associated with out-of-plane deformations and lateral torsional buckling. At larger drift amplitudes (i.e., 4% radians), columns that utilized cross-sections near λ_{hd} limits as per AISC (2010a) experience more than 50% reduction in their K_e regardless of the applied axial load ratio.
- Columns with larger member slenderness develop lower out-of-plane forces. CSA (2009) and AISC (2010b) highly overestimate the design brace force for columns with $L_b/r_y > 60$. The same standards have a small margin of safety against exceeding the design brace force for columns with $L_b/r_y < 45$. Furthermore, the FE investigation shows that out-of-plane force demands become smaller for higher compressive axial loads.
- A multivariate regression formulas is proposed to estimate the plastic hinge length in steel columns. Also a preliminary expression is proposed for estimating the out-of-plane force demands on the bracing member. The range of applicability of the proposed formulas are $12.1 \leq h/t_w \leq 57.5$, $44 \leq L_b/r_y \leq 120$, and $0 \leq P/P_y \leq 0.5$. These formulas can be adopted in future versions of CSA (2009) and AISC (2010b).

Based on these observations and in order to limit flexural strength deterioration to 80% M_p, flexural stiffness deterioration to 50% K_e, and axial shortening to 1% L at a chord-rotation of 4% radians, the following recommendations are proposed:

- A reduction to about two-thirds of the current compactness limit for highly ductile wide-flange cross-sections as per AISC (2010a) used in first story steel columns in steel MRFs.
- An upper limit of 30% P_y for the axial load in columns as part of steel special MRFs.
- Relaxing the current global slenderness ratio (L_b/r_y) for Type D MRFs as per (CSA 2009a) to 80. Additionally, Lower limits should be imposed for the warping and torsional constants (C_w and J). Preliminary limits of $C_w \geq 5.4 \times 10^{13}$ mm^6 and $J \geq 2.3 \times 10^7$ mm^4 are recommended for highly ductile columns. These limits are currently being refined.

References
ABAQUS-FEA/CAE (2011) Dassault Systemes Simulia Corp., RI, USA. © Dassault Systèmes, 2010.

AISC (2010a). "Seismic Provisions for Structural Steel Buildings", ANSI/AISC 341-10. American Institute for Steel Construction, Chicago, IL.

AISC (2010b). "Specification for Structural Steel Buildings", ANSI/AISC 360-10. American Institute for Steel Construction, Chicago, IL.

ASTM (2015). "Standard Specification for Structural Steel Shapes", ASTM A992 / A992M-11. ASTM International, West Conshohocken, PA, USA.

Bech, D., Tremayne, B. and Houston, J. (2015). "Proposed Changes to Steel Column Evaluation Criteria for Existing Buildings". *Proceedings of The 2nd ATC-SEI Conference on Improving the Seismic Performance of Existing Building and Other Structures*, San Francisco, CA, USA, December 10-12, 2015.

Chen, Y. Y., Niu, L. and Cheng, X. (2014). "Hysteretic Behaviour of H Steel Columns with Large Width-Thickness Ratios under Bi-Axis Moments". *Proceedings of The 10th National Conference on Earthquake Engineering (10NCEE)*, Anchorage, Alaska, July 21-25, 2014.

Clark, P., Frank, K., Krawinkler, H. and Shaw, R. (1997). "Protocol for Fabrication, Inspection, Testing, and Documentation of Beam-Column Connection Tests and Other Experimental Specimens", Report No. SAC/BD-97. SAC Joint Venture.

CSA (2009). "Design of Steel Structures", CAN/CSA S16-09. Canadian Standards Association, Mississauga, Canada.

Elkady, A. and Lignos, D. G. (2014). "Modeling of the Composite Action in Fully Restrained Beam-to-Column Connections: Implications in the Seismic Design and Collapse Capacity of Steel Special Moment Frames". *Earthquake Engineering & Structural Dynamic*; 43 (13) 1935-1954. DOI: 10.1002/eqe.2430.

Elkady, A. and Lignos, D. G. (2015a). "Analytical Investigation of the Cyclic Behavior and Plastic Hinge Formation in Deep Wide-Flange Steel Beam-Columns". *Bulletin of Earthquake Engineering*; 13 (4) 1097-1118. DOI: 10.1007/s10518-014-9640-y.

Elkady, A. and Lignos, D. G. (2015b). "Effect of Gravity Framing on the Overstrength and Collapse Capacity of Steel Frame Buildings with Perimeter Special Moment Frames". *Earthquake Engineering & Structural Dynamic*; 44 (8) 1289–1307. DOI: 10.1002/eqe.2519.

Elkady, A. (2016). "Collapse Risk Assessment of Steel Moment Resisting Frames Designed with Deep Wide-Flange Columns in Seismic Regions". McGill University, Canada.

Elkady, A. and Lignos, D. G. (2016). "Dynamic Stability of Deep and Slender Wide-Flange Steel Columns – Full Scale Experiments". *Proceedings of The Annual Stability Conference*, Orlando, Florida, USA, April 12-15, 2016.

Elkady, A. and Lignos, D. G. (2017). "Full-Scale Cyclic Testing of Deep Slender Wide-Flange Steel Beam-Columns under Unidirectional and Bidirectional Lateral Drift Demands". *Proceedings of The 16th World Conference on Earthquake Engineering*, Santiago, Chile, January 9-13, 2017.

Kemp, A. R. (1996). "Inelastic Local and Lateral Buckling in Design Codes". *Journal of Structural Engineering*; 122 (4) 374-382

Krawinkler, H. (2009). "Loading Histories for Cyclic Tests in Support of Performance Assessment of Structural Components". *Proceedings of The 3rd International Conference on Advances in Experimental Structural Engineering*. pp 15-16

Lignos, D. G., Hikino, T., Matsuoka, Y. and Nakashima, M. (2013). "Collapse Assessment of Steel Moment Frames Based on E-Defense Full-Scale Shake Table Collapse Tests". *Journal of Structural Engineering*; 139 (1) 120-132. DOI: 10.1061/(ASCE)ST.1943-541X.0000608.

Lignos, D. G., Cravero, J. and Elkady, A. (2016). "Experimental Investigation of the Hysteretic Behavior of Wide-Flange Steel Columns Under High Axial Load And Lateral Drift Demands". *Proceedings of The 11th Pacific Structural Steel Conference*, Shanghai, China, October 26-28, 2016.

MacRae, G. A., Carr, A. J. and Walpole, W. R. (1990). "The Seismic Response of Steel Frames", Report No. 90-6. Department of Civil Engineering, University of Canterbury, New Zealand.

Nakashima, M., Takanashi, K. and Kato, H. (1990). "Test of Steel Beam-Columns Subject to Sidesway". *Journal of Structural Engineering*; 116 (9) 2516-2531

Newell, J. D. and Uang, C.-M. (2006). "Cyclic Behavior of Steel Columns with Combined High Axial Load and Drift Demand", Report No. SSRP-06/22. Department of Structural Engineering, University of California, San Diego.

NIST (2010). "Research Plan for the Study of Seismic Behaviour and Design of Deep Slender Wide Flange Structural Steel Beam-Column Members", NIST GCR 11-917-13. NEHRP consultants Joint Venture.

Popov, E. P., Bertero, V. V. and Chandramouli, S. (1975) Hysteretic Behavior of Steel Columns. Earthquake Engineering Research Center, University of California,

Suzuki, Y. and Lignos, D. G. (2014). "Development of Loading Protocols for Experimental Testing of Steel Columns Subjected to Combined High Axial Load and Lateral Drift Demands Near Collapse". *Proceedings of*

10th National Conference on Earthquake Engineering (10th NCEE), Anchorage, Alaska, USA, July 21-25, 2014. DOI:10.4231/D3M32N99R.

Suzuki, Y. and Lignos, D. G. (2015). "Large Scale Collapse Experiments of Wide Flange Steel Beam-Columns". *Proceedings of The 8th International Conference on Behavior of Steel Structures in Seismic Areas (STESSA)*, Shanghai, China, July 1-3, 2015.

Uang, C.-M., Ozkula, G. and Harris, J. (2015). "Observations from Cyclic Tests on Deep, Slender Wide-Flange Structural Steel Beam-Column Members". Paper presented at the The Annual Stability Conference, Structural Stability Research Council (SSRC), Nashville, Tennessee, USA, March 24-27, 2015.